Geochemistry Geophysics Geosystems G3
AN ELECTRONIC JOURNAL OF THE EARTH SCIENCES
Published by AGU and the Geochemical Society

Article
Volume 4, Number 12
2 December 2003
1098, doi:10.1029/2003GC000585
ISSN: 1525-2027

Millennial-scale variability of deep-water temperature and $\delta^{18}O_{dw}$ indicating deep-water source variations in the Northeast Atlantic, 0–34 cal. ka BP

L. C. Skinner and N. J. Shackleton
Godwin Institute for Quaternary Research, Department of Earth Sciences, University of Cambridge, New Museums Site, Pembroke Street, Cambridge, CB2 3SA, UK (luke00@esc.cam.ac.uk)

H. Elderfield
Department of Earth Sciences, University of Cambridge, Downing Street, Cambridge, CB2 3EQ, UK

[1] Paired measurements of Mg/Ca and $\delta^{18}O_{cc}$ (calcite $\delta^{18}O$) in benthic foraminifera from a deep-sea core recovered on the Iberian Margin (MD99-2334K; 37°48′N, 10°10′W; 3,146 m) have been performed in parallel with planktonic $\delta^{18}O_{cc}$ analyses and counts of ice-rafted debris (IRD). The synchrony of temperature changes recorded in the Greenland ice cores and in North Atlantic planktonic $\delta^{18}O_{cc}$ allows the proxy records from MD99-2334K to be placed confidently on the GISP2 time-scale. This correlation is further corroborated by AMS ^{14}C-dates. Benthic Mg/Ca measurements in MD99-2334K permit the reconstruction of past deep-water temperature (T_{dw}) changes since ~34 cal. ka BP (calendar kiloyears before present). Using these T_{dw} estimates and parallel benthic $\delta^{18}O_{cc}$ measurements, a record of deep-water $\delta^{18}O$ ($\delta^{18}O_{dw}$) has been calculated. Results indicate greatly reduced T_{dw} in the deep Northeast Atlantic during the last glaciation until ~15 cal. ka BP, when T_{dw} warmed abruptly to near-modern values in parallel with the onset of the Bølling-Allerød interstadial. Subsequently, T_{dw} reverted to cold glacial values between ~13.4 and ~11.4 cal. ka BP, in parallel with the Younger Dryas cold reversal and the H0 ice-rafting event. Similar millennial-scale T_{dw} changes also occurred during the last glaciation. Indeed, throughout the last ~34 cal. ka, millennial $\delta^{18}O_{dw}$ and T_{dw} changes have remained well coupled and are linked with IRD pulses coincident with Heinrich events 3, 2, 1, and the Younger Dryas, when transitions to lower T_{dw} and $\delta^{18}O_{dw}$ conditions occurred. In general, millennial T_{dw} and $\delta^{18}O_{dw}$ variations recorded in MD99-2334K describe an alternation between colder, low-$\delta^{18}O_{dw}$ and warmer, high $\delta^{18}O_{dw}$ conditions, which suggests the changing local dominance of northern-sourced North Atlantic Deep Water (NADW) versus southern-sourced Antarctic Bottom Water (AABW). The observed similarity of the T_{dw} and GISP2 $\delta^{18}O_{ice}$ records would therefore suggest a common component of variability resulting from the coupling of NADW formation and Greenland climate. A link between Greenland stadials and the incursion of cold, low-$\delta^{18}O_{dw}$ AABW in the deep Northeast Atlantic is thus implied, which contributes to the relationship between Greenland climate and the millennial benthic $\delta^{18}O_{cc}$ signal since ~34 cal. ka BP.

Components: 8774 words, 8 figures, 1 table.

Keywords: Deep-water temperature; Mg/Ca; Termination I; thermohaline circulation.

Index Terms: 4267 Oceanography: General: Paleoceanography; 4875 Oceanography: Biological and Chemical: Trace elements; 4870 Oceanography: Biological and Chemical: Stable isotopes.

Received 9 June 2003; **Revised** 30 September 2003; **Accepted** 13 October 2003; **Published** 2 December 2003.

Skinner, L. C., N. J. Shackleton, and H. Elderfield, Millennial-scale variability of deep-water temperature and $\delta^{18}O_{dw}$ indicating deep-water source variations in the Northeast Atlantic, 0–34 cal. ka BP, *Geochem. Geophys. Geosyst.*, *4*(12), 1098, doi:10.1029/2003GC000585, 2003.

1. Introduction

[2] The synchrony of millennial-scale climate change recorded in the Greenland ice cores and North Atlantic marine sediments [*Broecker*, 1994] contrasts with the distinct asynchrony that has been identified between planktonic and benthic foraminiferal calcite $\delta^{18}O$ ($\delta^{18}O_{cc}$) in the North Atlantic (40–60 cal. ka BP (calendar kiloyears before present)) [*Shackleton et al.*, 2000], which in turn is set to the phasing of Greenland and Antarctic millennial-scale temperature change [*Blunier et al.*, 1998; *Blunier and Brook*, 2001]. The coupling of Greenland and North Atlantic temperatures has long been proposed to involve perturbations to the thermohaline circulation system, which may behave in an ''oscillatory'' manner, alternating between stability modes characterised by the dominance of either northern- or southern sourced deep-water in the deep Atlantic [e.g., *Duplessy et al.*, 1988; *Charles et al.*, 1996; *Boyle*, 2000], and potentially responding to internal instabilities and/or external forcing (such as ice dynamics and/or ice-volume fluctuations) initiated in either hemisphere [e.g., *Stocker et al.*, 1992; *Broecker*, 1994; *Kanfoush et al.*, 2000; *Seidov and Maslin*, 2001; *Weaver et al.*, 2003]. If so, the changes in deep-water hydrography that would accompany such thermohaline perturbations, including changes in local deep-water temperature (T_{dw}) and deep-water $\delta^{18}O$ ($\delta^{18}O_{dw}$), will have left their mark on the benthic $\delta^{18}O_{cc}$ record, thereby influencing the millennial benthic $\delta^{18}O_{cc}$ signal and its apparent relationship to North Atlantic surface climate.

[3] The relatively recent advent of Mg/Ca-palaeothermometry in foraminiferal calcite [*Nürnberg*, 1995; *Nürnberg et al.*, 1996b; *Rosenthal et al.*, 1997; *Lea et al.*, 1999; *Mashiotta et al.*, 1999; *Elderfield and Ganssen*, 2000; *Lea et al.*, 2000; *Lear et al.*, 2000; *Martin et al.*, 2002] presents the possibility of constraining the temperature component of foraminiferal $\delta^{18}O_{cc}$, provided secondary influences on Mg/Ca such as dissolution and/or contamination may be eliminated and a suitable Mg/Ca-temperature calibration may be obtained. In this way, the deep-water temperature component of the benthic $\delta^{18}O_{cc}$ record may be separated from the combined contributions of glacioeustacy and local deep-water $\delta^{18}O$ change. Here, parallel $\delta^{18}O_{cc}$ and Mg/Ca analyses have been made on the benthic species *Globobulimina affinis* in core MD99-2334K (recovered from the Iberian Margin; 37°48′N, 10°10′W; 3,146 m) in order to estimate the deep-water temperature component of the Northeast Atlantic benthic $\delta^{18}O_{cc}$ record during the end of the last glaciation and across Termination I. At the location of MD99-2334K, it has been shown that the infaunal benthic species *G. affinis* exhibits a constant $\delta^{18}O$ offset with respect to *Uvigerina peregrina* and *Planulina wuellerstorfii* [*Shackleton et al.*, 2000]. Hence despite its infaunal habitat, *G. affinis* must have experienced and recorded the same environmental controls on $\delta^{18}O_{cc}$ as *P. wuellerstorfii* and *U. peregrina*.

[4] The location of core MD99-2334K and the modern deep hydrography on the Iberian Margin are shown in Figure 1. At present, the site of MD99-2334K is bathed in northward re-circulating Northeast Atlantic Deep Water (NEADW), a ''derivative'' of North Atlantic Deep Water (NADW) that presently includes ~47% Lower Deep Water (LDW), which is derived from Antarctic Bottom Water (AABW) [*van Aken*, 2000]. The core site is therefore well situated to record past changes in NADW export and AABW incursion into the deep North Atlantic.

2. Methods

[5] Benthic foraminifera (*P. wuellerstorfii* and *G. affinis*) were picked from the >212 μm coarse fraction of sediment samples, which were disaggregated using de-ionised water. As many foraminifera as possible were picked (on average ~20

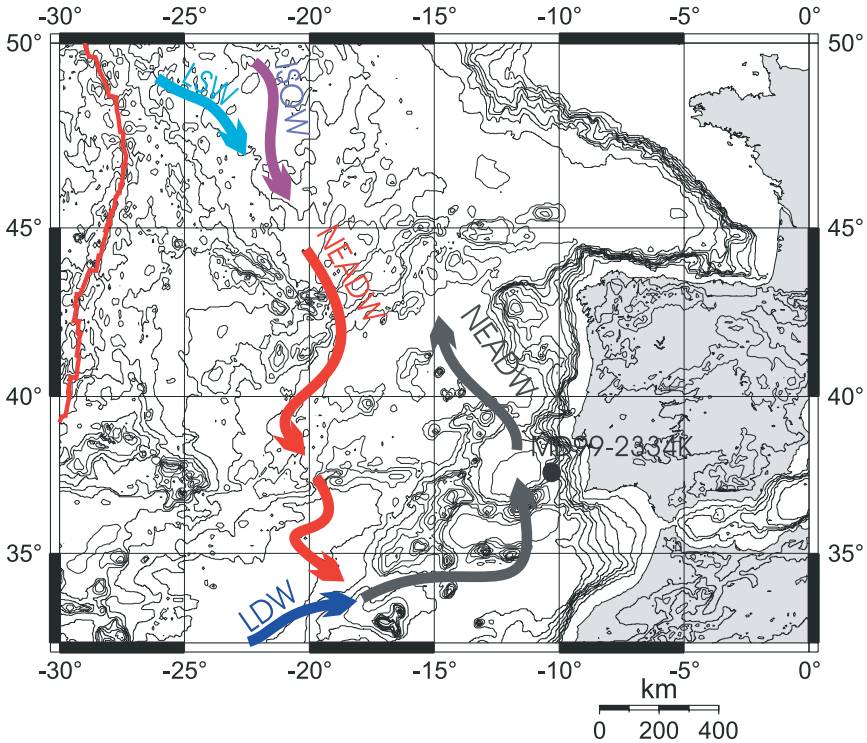

Figure 1. Location map for core MD99-2334K, on the Iberian Margin in the Northeast Atlantic (37°48′N, 10°10′W; 3,146 m), summarizing the modern local deep-water hydrography as derived primarily from *van Aken* [2000]. Core MD95-2042 [*Shackleton et al.*, 2000] is also from the same location. The red line indicates position of Mid-Atlantic Ridge. The main deep water mass in the deep Northeast Atlantic basin is Northeast Atlantic Deep Water (NEADW), which is derived from four main end-members: (1) Labrador Seawater (LSW), a relatively fresh and cold intermediate/deep water mass formed in the Labrador Sea through winter convection; (2) Iceland-Scotland Overflow Water, a deep water mass derived from Nordic Seawater mixed with LSW and entrained sub-polar intermediate water; (3) Mediterranean Seawater (MSW), a warm and very saline water mass circulating at intermediate depths; and (4) Lower Deep Water (LDW), a southern-sourced abyssal water mass derived from Antarctic Bottom Water (AABW). Below ~3,000 m, recirculating modern NEADW thus comprises ~47% LDW, ~27% ISOW, ~23% LSW and ~3% MSW (T_{dw} ~ 2.8°C, $\delta^{18}O_{dw}$ ~ 0.2‰).

G. affinis and ~3 *P. wuellerstorfii*) in order to reduce statistical variability and so that sample concentrations for Mg/Ca analysis were maintained as high as possible (ideally $[Ca^{++}]$ ~ 100 ppm, though ~40 ppm on average). *P. wuellerstorfii* was sampled for stable isotope measurements, and *G. affinis* was sampled for parallel stable isotope and Mg/Ca measurements. In addition, ~30 specimens of *Globigerina bulloides* were picked from the 250–300 μm size fraction of each sample interval for stable isotope analyses, and counts of terrigenous clastic material (indicative of ice-rafted debris) were made on material >90 μm.

[6] After being crushed between clean glass plates, samples of *G. affinis* were homogenised and cleaned, and then split into separate aliquots for isotope and minor element analyses. This ensured that isotopic and minor element measurements were made on the same samples of cleaned calcite, and eliminated potential discrepancies due to the effects of different cleaning methods on measured Mg/Ca and $\delta^{18}O$. However, when specimens were too sparse and hence samples were too small to be split between Mg/Ca and $\delta^{18}O$ analyses, the samples were used for either isotope or minor element analysis only. The Mg/Ca cleaning process is after *Barker et al.* [2003] and involved: (1) repeated clay removal in ultra-pure de-ionised water by ultrasonification, agitation and subsequent settling with removal of water; (2) removal of organic material by oxidation in 500 μl 30% w/v Aristar grade H_2O_2

with 15 ml 0.1M NaOH (heated to ~90°C for 10 minutes in total), followed by rinsing; (3) weak acid leach using 0.001M HNO_3, followed by rinsing; and finally (4) dissolution in 0.075M HNO_3, settling out of any less soluble impurities that may remain, and transferral to a clean vial just prior to analysis. Concentrations of sample solutions were modified so that [Ca^{++}] was ideally 40–70 ppm, and intensity calibrations were carried out following *de Villiers et al.* [2002] in order to limit ''matrix effects''. Routine consistency standards analysed in parallel with sample measurements were reproducible on the long-term to significantly better than 1.0% relative standard deviation (RSD). However the identification of a blank contamination effect equivalent to ~1.8 ppb Mg (derived from the leaching of plastic vials and bottles used for reagent and sample storage) means that, for the average concentration and Mg/Ca of the samples analysed ([Ca^{++}] ~ 40 ppm, Mg/Ca ~ 2.75 mmol mol^{-1}), a relative error of ~+2.5% may be expected. No attempt has been made in this study to correct for the expected blank error (equivalent to ~0.08 mmol mol^{-1} excess Mg/Ca on average). Instead, it is incorporated into the Mg/Ca-temperature calibration proposed below, and therefore effectively removed from temperature reconstructions. All minor element analyses were carried out on an ICP-AES (Varian Vista) as described by *de Villiers et al.* [2002]. Stable isotope analyses were carried out on a Micromass Multicarb Sample Preparation System attached to a PRISM mass spectrometer (or attached to a SIRA mass spectrometer for the larger *G. bulloides* samples). Measurements of $\delta^{18}O$ were determined relative to the Vienna Peedee Belemnite (VPDB) standard, and the analytical precision was better than 0.08‰.

3. Mg/Ca–Temperature Calibration

[7] The exponential temperature-dependence of Mg-uptake in foraminifera is being established with increasing confidence [*Nürnberg*, 1995; *Nürnberg et al.*, 1996b; *Rosenthal et al.*, 1997; *Lea et al.*, 1999; *Mashiotta et al.*, 1999; *Elderfield and Ganssen*, 2000; *Lea et al.*, 2000; *Lear et al.*, 2000, 2002; *Martin et al.*, 2002; *Anand et al.*, 2003]. The most recent benthic calibration for Mg/Ca-temperature has been carried out by *Lear et al.* [2002], incorporating data from the previous study of *Martin et al.* [2002], and indicating a large degree of inter-species variability in Mg-uptake, though relatively minor variability in Mg/Ca temperature-sensitivity. Currently, there is no published Mg/Ca - temperature calibration for *G. affinis*, and there are no specimens in the Holocene portion of core MD99-2334K that may be used for calibration. However, it has been shown that Mg/Ca in living specimens of *G. affinis* from the Bay of Biscay do indeed exhibit a clear correlation with variations in deep-water temperature [*Tachikawa et al.*, 2003].

[8] In order to construct a specific calibration for *G. affinis*, an exponential relationship may be solved for robust estimates of high and low temperature - Mg/Ca boundary conditions. Many lines of evidence suggest that deep-water temperatures are likely to have approached the freezing limit during the last glaciation [e.g., *Labeyrie et al.*, 1987; *Zahn and Mix*, 1991; *Dwyer et al.*, 2000; *Duplessy et al.*, 2002; *Martin et al.*, 2002; *Schrag et al.*, 2002], providing a lower temperature limit for calibration against minimum glacial Mg/Ca ratios in MD99-2334K (14 measurements, see Figure 5). The in situ freezing temperature for a water depth of 3,146 m is ~−1.8°C. During the last interglacial, Marine Isotope Stage (MIS) 5e, T_{dw} on the Iberian Margin cannot have differed from modern temperatures by more than ~+0.48°C. This estimate is based on the similarity of MIS 1 and MIS 5e sea levels (up to ~5 m higher during MIS 5e) [*Edwards et al.*, 1997; *Stirling et al.*, 1998; *Lambeck and Chappell*, 2001; *Gallup et al.*, 2002] and benthic $\delta^{18}O_{cc}$ (~0.15‰ lower during MIS 5e) [*Shackleton et al.*, 2003]. Given a 0.008‰ change in mean ocean $\delta^{18}O_{dw}$ per meter sea level rise [*Adkins et al.*, 2002], and a 0.23‰ $°C^{-1}$ temperature effect [*O'Neil et al.*, 1969; *Shackleton*, 1974], MIS 5e T_{dw} must have been ~0.48°C warmer (i.e., ~3.28°C). Hence 3.28°C may be used for calibration against 8 Mg/Ca measurements in *G. affinis* that have been obtained for MIS 5e from a neighboring piston core MD01-2444 (L. C. Skinner, unpublished data, 2003).

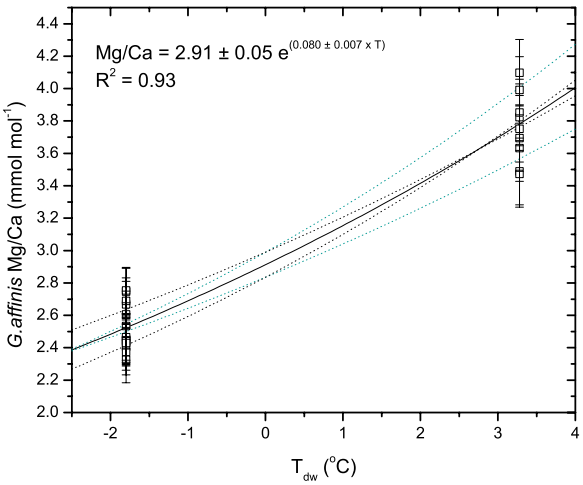

Figure 2. Mg/Ca - temperature calibration proposed for *G. affinis*, based on minimum glacial Mg/Ca measurements calibrated against local freezing temperature (−1.6°C) and Mg/Ca measurements from MIS 5e, made in adjacent core MD01-2444, calibrated against modern temperatures +1.4°C (see text). Error bars on measurements represent 1σ for 14 measurements from MD99-2334K (glacial) and 8 measurements from MD01-2444 (MIS 5e). Dashed lines represent the 2σ uncertainty in the calibration parameters, derived by propagation of errors.

Fitting an exponential Mg/Ca – temperature relationship of the form $Mg/Ca = Ae^{(b\times T)}$ to the Mg/Ca data available for the assumed boundary conditions yields the calibration (see Figure 2):

$$Mg/Ca = 2.91 \pm 0.05 \times e^{(0.080\pm0.007\times T)}$$

(Errors represent 1σ.)

$$R^2 = 0.93$$

[9] Work on the temperature calibration of Mg/Ca in planktonic foraminifera is at a much more advanced stage than for benthic foraminifera, and it is notable that the temperature sensitivity of most planktonic species appears to converge on a single value of ∼10% change in Mg/Ca per °C, while the pre-exponential constant (or absolute Mg/Ca levels) may vary more substantially between species [*Anand et al.*, 2003]. The same can be said for the benthic species studied to date, and it is also notable that previous studies suggest no consistent difference in the Mg/Ca-temperature sensitivity of infaunal versus epifaunal benthic taxa [*Rosenthal et al.*, 1997; *Lear et al.*, 2002; *Martin et al.*, 2002]. Hence the "slope" of Mg/Ca-temperature calibrations in foraminiferal calcite is a robust feature, generally ∼0.1. This is consistent with the slope obtained for the *G. affinis* calibration (∼0.08), which is intermediate with respect to published calibrations for both epifaunal and infaunal benthic species (ranging from ∼0.061 to ∼0.150) [*Rosenthal et al.*, 1997; *Lear et al.*, 2002; *Martin et al.*, 2002]. The pre-exponential factor in the *G. affinis* calibration (∼2.91) is much larger than for other benthic and planktonic calibrations [*Rosenthal et al.*, 1997; *Lear et al.*, 2002; *Martin et al.*, 2002; *Anand et al.*, 2003], however there can be little doubt that this is required by the fact that *G. affinis* exhibits relatively elevated Mg/Ca ratios, which are up to four times higher than coexisting *P. wuellerstorfii* [*Tachikawa et al.*, 2003], and often higher than many planktonic species despite its low-temperature benthic habitat.

[10] Hence the proposed Mg/Ca-temperature calibration for *G. affinis* is supported by three strong arguments: (1) the observed temperature response of Mg/Ca measured in living *G. affinis* specimens [*Tachikawa et al.*, 2003]; (2) the consistency of the proposed calibration "slope" with that almost universally observed in foraminiferal calcite; and (3) the necessary constraints placed on the pre-exponential constant of any calibration for *G. affinis*, given its elevated Mg-content relative to both planktonic and other benthic species. The uncertainty limits quoted above for the proposed calibration are estimated based on the variance of the data required for its generation (2σ level), however a significantly greater "empirical" uncertainty must be qualified. In estimating the uncertainty inherent in down-core temperature records (see below) a distinction is made between the uncertainty inherent in down-core Mg/Ca measurements and the additional uncertainty resulting from the derivation of T_{dw}. Sensitivity tests indicate that the main implications drawn from the Mg/Ca record obtained from MD99-2334K are not affected by the estimated uncertainties in the temperature calibration parameters, however the absolute temperatures that it generates remain to be tested against a modern data set. This is particularly important

for the lower temperature range, which has been calibrated against a minimum (near-freezing) temperature limit.

[11] In the above calibration and throughout this paper, "deep-water temperature" (T_{dw}) refers to in situ temperatures, as opposed to potential temperatures. Although potential temperature, which is a conservative measurement, is generally used for the purposes of oceanographic description, it is the in situ temperature that is "experienced" by foraminifera.

4. Dissolution and Contamination

[12] Diagenetic dissolution would be expected to reduce the Mg/Ca of foraminiferal calcite as well as the average foram shell weight, and would be expected to have a greater effect on planktonic species, both because benthics are more resistant to dissolution and because the planktonic life cycle results in an uneven distribution of Mg in planktonic tests, with Mg-rich calcite being more prone to dissolution [*Brown and Elderfield*, 1996]. It can be shown that planktonic foraminifera in core MD99-2334K have not been subject to significant diagenetic dissolution, as their Mg/Ca ratios are negatively correlated with both Sr/Ca and average planktonic shell weights (L. C. Skinner, unpublished data, 2003), all of which would be reduced by dissolution [*Brown and Elderfield*, 1996]. Benthic foraminifera could not have been dissolved while planktonic foraminifera remained unaffected, and hence diagenetic dissolution does not appear to represent a significant control on the variability of benthic Mg/Ca ratios, as for planktonic Mg/Ca ratios. Ratios of Fe/Ca, Mn/Ca and Al/Ca serve as indicators of potential contamination of Mg/Ca measurements by Mg-bearing clays and/or authigenic encrustations. These secondary metal ratios exhibit no positive correlation with Mg/Ca measured in *G. affinis*, and therefore suggest that contamination is not a significant control on Mg/Ca variability (Figure 3). If it is assumed that the measured "contaminant" metals are representative of a silicate phase, then for a typical silicate Mg/Fe ratio of ~1 mol mol^{-1}, only ~10% of the measured Mg/Ca in *G. affinis* (i.e., ~0.25 mmol mol^{-1}, or ~1°C) could be attributed to contamination. This is approximately equivalent to the estimated uncertainty in the *G. affinis* Mg/Ca record, as described below. However, it is probable that most of the contaminant metals are in fact associated with a ferromanganese carbonate overgrowth [*Boyle*, 1983], particularly given the elevated Mn/Ca ratios observed, and given also the fact that Al is actually below satisfactory detection limits in all of the samples analysed. For a typical deep marine ferromanganese precipitate Mg/Mn ratio of ~0.1 mol mol^{-1} [*de Lange et al.*, 1992], one may expect a contamination effect on measured Mg/Ca ratios equivalent to ~0.08 mmol mol^{-1} or ~0.3°C (significantly less than the estimated uncertainty in the Mg/Ca record of *G. affinis*).

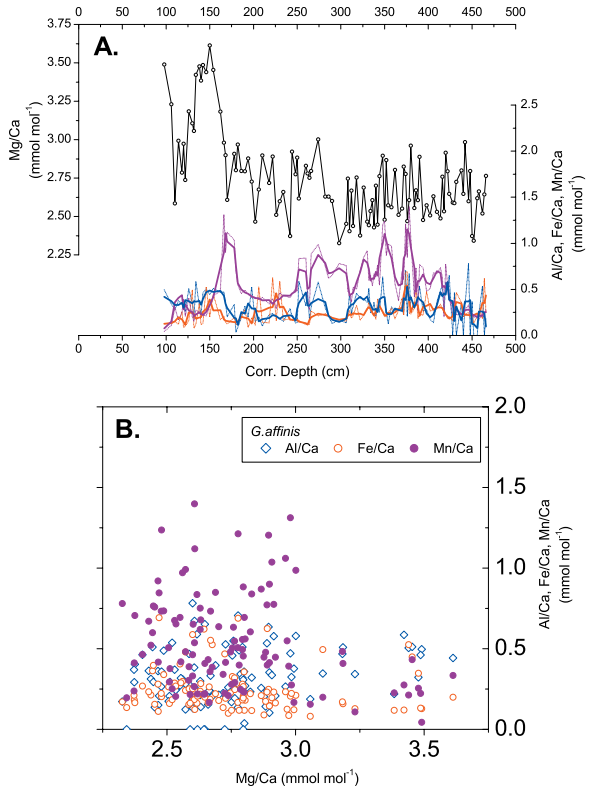

Figure 3. Minor element content of *G. affinis* samples analysed for Mg/Ca. (a) Down-core measurements of Mg/Ca in *G. affinis* (black line, open circles), compared with Mn/Ca (purple), Fe/Ca (orange) and Al/Ca (blue), all measured in parallel with Mg/Ca. (b) Scatter of Fe/Ca, Mn/Ca and Al/Ca plotted against Mg/Ca, showing no covariance between these metals.

[13] The contribution of primary controls other than temperature (such as salinity or pore water pH) on the Mg-uptake of *G. affinis* is difficult to

assess, however studies to date suggest that such environmental factors are generally overwhelmed by the effects of temperature, particularly over the range of salinity and pH that may be reasonably expected in the deep marine environment [*Nürnberg et al.*, 1996a; *Lea et al.*, 1999; *Rosenthal et al.*, 2000; *Toyofuku et al.*, 2000]. The environmental sensitivity of Mg-uptake into foraminiferal calcite remains an area of continuing research, which may yet reveal a wide range of environmental controls that operate at lower temperatures and/or at low foraminiferal Mg/Ca ratios in particular. In this study, although the contribution of small absolute inaccuracies due to minor partial dissolution and/or contamination, or of secondary and as yet unknown environmental controls on Mg-uptake cannot be unequivocally ruled out, temperature must be assumed to be the dominant control on Mg/Ca variability in *G. affinis*.

5. Core Chronology

[14] The age-model for the core has been derived based on the synchrony of rapid warming events recorded in the North Atlantic planktonic $\delta^{18}O_{cc}$ record and in the GISP2 Greenland ice core $\delta^{18}O_{ice}$ record [*Shackleton et al.*, 2000]. The resulting GISP2 age-model based on correlation (using the age-scale of *Meese et al.* [1997]) is corroborated by AMS ^{14}C-dating (performed at LSCE, Gif-sur-Yvette), using monospecific samples of *Neogloboquadrina pachyderma* and *Globigerina bulloides* taken from local species abundance maxima in order to limit the influence of bioturbation [*Bard et al.*, 1987]. Calibration of the ^{14}C-dates to calendar years has been performed using a second order polynomial equation fit to data from *Bard et al.* [1990] and from *Voelker et al.* [2000]. The correlation with GISP2 and the resulting sedimentation rates are shown in Figures 4a–4e. The inferred timing of ice-rafted debris (IRD) pulses recorded in MD99-2334K, which coincide with Heinrich events 3, 2, 1 and the Younger Dryas (H0), is shown in Figure 4d, lending further support for the GISP2 correlation. A comparison between calibrated ^{14}C-ages and correlative GISP2 ages is made in Figure 4e, indicating a linear relationship that is indistinguishable from 1:1 at the 95% confidence level. Correlative core depths, ^{14}C ages, calendar ages and age offsets are summarized in Table 1.

6. Results and Discussion

6.1. Down-Core Trends

[15] Figure 5 illustrates the down-core Mg/Ca-temperature, stable isotope and IRD concentration results on the GISP2 age-scale, with the GISP2 $\delta^{18}O_{ice}$ record shown for comparison. In order to remove from the benthic $\delta^{18}O_{cc}$ record the component that is due to T_{dw} variations, the palaeotemperature equation of *O'Neil et al.* [1969] [*O'Neil et al.*, 1969; *Shackleton*, 1974] has been applied, yielding a record of deep-water $\delta^{18}O$ ($\delta^{18}O_{dw}$) that combines the effects of both glacioeustacy and local water mass variability. The similarity of many features in the $\delta^{18}O_{dw}$ and $\delta^{18}O_{cc}$ records lends support to the $\delta^{18}O_{dw}$ reconstruction. The overall uncertainty in the $\delta^{18}O_{cc}$ record has been estimated as twice the mean standard deviation of successive measurement pairs; equivalent to $\sim\pm0.1$‰, which exceeds the analytical measurement precision. The same approach has been adopted in order to estimate the down-core uncertainty in the Mg/Ca measurements, which is equivalent to $\sim\pm0.14$ mmol mol^{-1} and which also greatly exceeds the estimated analytical precision. This uncertainty has been combined with the 2σ limits estimated for the temperature calibration parameters, and propagated to the calculated T_{dw} record, yielding a down-core uncertainty of $\sim\pm0.7$°C. The uncertainty thus inferred for the T_{dw} and $\delta^{18}O_{cc}$ records has been propagated to the calculated $\delta^{18}O_{dw}$ record. 3-point smoothed records reduce all uncertainties (and interpretable variations in the data) proportionately, and t-tests for the significant difference of means, carried out for 5-point runs of data points, define changes in the records that are statistically significant with respect to their inherent uncertainties, using a 90% two-tailed confidence interval. The most salient and robust aspects of the records are thus distinguished, and although the absolute magnitudes of the identified T_{dw} and $\delta^{18}O_{bw}$ changes are dependant on the calibration assumptions, they nevertheless remain significant qualitative features of the record with

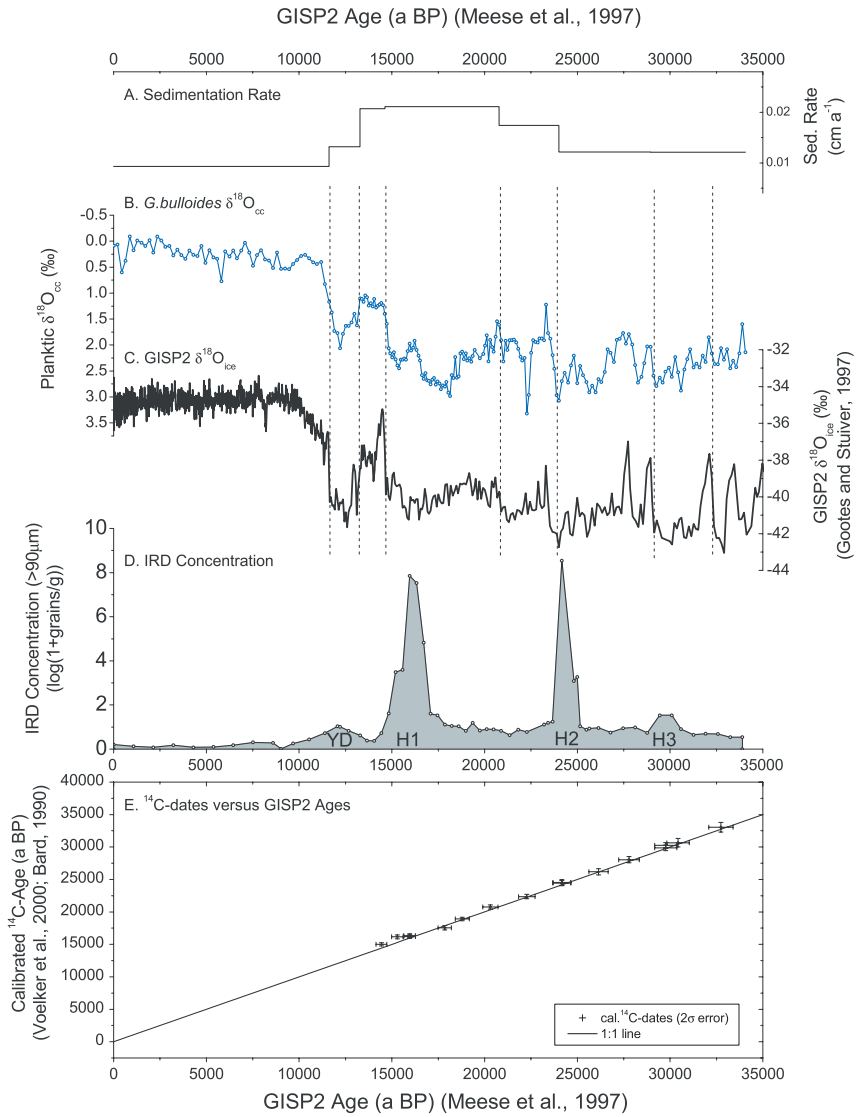

Figure 4. Age-model for core MD99-2334K, based on synchrony of temperature changes recorded in planktonic $\delta^{18}O_{cc}$ and GISP2 $\delta^{18}O_{ice}$, and corroborated by ^{14}C-dating. (a) Changes in sedimentation rate defined by age tie-points. (b) Planktonic $\delta^{18}O_{cc}$ measured in *G. bulloides* (250–300 μm) from MD99-2334K. (c) GISP2 $\delta^{18}O_{ice}$ record [*Grootes and Stuiver*, 1997] used for correlation with planktonic $\delta^{18}O_{cc}$ record, yielding age-model on GISP2 age-scale [*Meese et al.*, 1997]. (d) Concentration of terrigenous clastics counted in >90 μm fraction, taken as indication of local IRD deposition. IRD peaks correspond to peak Greenland stadials that accompany Heinrich events 3, 2, 1, and the Younger Dryas. (e) Comparison of calibrated ^{14}C-ages with correlative GISP2 ages derived from correlation. Calibration of ^{14}C ages (~12–35 ^{14}C ka BP) is based on second order polynomial fit to data from *Bard et al.* [1990] and *Voelker et al.* [2000], giving preference to coral dates prior to ~20 ^{14}C ka BP. For ^{14}C ages ~12–35 ka BP, using a constant reservoir age of 400 years: Calendar Age = $-2.12108 + 1.48538(^{14}C_{age}) - 0.00967(^{14}C_{age})^2$; $R^2 = 0.994$. The paired dates describe a linear relationship that is indistinguishable from 1:1 at the 95% confidence level.

respect to the estimated uncertainties in both the down-core results and the Mg/Ca - T_{dw} calibration.

6.2. Millennial-Scale Climate Associations

[16] The benthic Mg/Ca-temperature record from MD99-2334K indicates that throughout the last glaciation, since ~34 cal. ka BP, deep-water temperatures in the Northeast Atlantic were markedly reduced, remaining well below the modern interglacial temperature of ~2.8°C (Figure 5). At ~15 cal. ka BP, coincident with the beginning of the Bølling-Allerød interstadial,

Table 1. Core Depths, ^{14}C-Ages, Calibrated ^{14}C-Ages, and Corresponding GISP2 Ages Based on Stratigraphic Correlation (See Figure 2)[a]

MD99-2334K Corrected Depth, cm	Species	^{14}C Age, ^{14}C-Years[b]	^{14}C Error, 1σ Years	Calibrated ^{14}C-Age,[c] cal. Years	Cal. ^{14}C Error, 1σ Years	GISP2 Correlative Age, Years	GISP2 Error,[d] 1σ Years	GISP2 – cal. ^{14}C Age Offset, Years
154	G. bull	12,960	110	15,010	130	14,438	289	−572
172	G. bull	13,890	130	16,157	153	15,293	306	−864
186	G. bull	13,920	110	16,194	129	15,956	319	−238
186	N. pach	14,050	120	16,353	141	15,956	319	−397
226	N. pach	15,050	140	17,564	163	17,848	357	284
246	G. bull	16,180	120	18,910	138	18,795	376	−116
278	G. bull	17,780	140	20,774	159	20,309	406	−465
314	G. bull	19,170	150	22,353	169	22,276	446	−77
346	G. bull	21,160	190	24,548	210	24,165	483	−383
346	N. pach	21,070	180	24,450	199	24,165	483	−286
370	G. bull	22,700	220	26,194	239	26,141	523	−53
390	G. bull	24,480	220	28,040	236	27,788	556	−252
414	G. bull	26,310	200	29,873	211	29,767	595	−106
414	N. pach	26,710	200	30,266	210	29,767	595	−499
422	G. bull	27,110	310	30,655	324	30,428	609	−227
450	G. bull	29,640	360	33,044	367	32,741	655	−303

[a] Age offsets between correlative GISP2 ages and calibrated ^{14}C-ages are also shown, all within error of zero.
[b] Corrected for 400 year reservoir effect.
[c] *Bard* [1990] and *Voelker et al.* [2000].
[d] *Meese et al.* [1997].

T_{dw} warmed abruptly by ~3°C. Subsequently, between ~13.4 and 11.4 cal. ka BP, T_{dw} reverted to cold glacial temperatures, coincident with the Younger Dryas cold reversal and the H0 ice-rafting event. Hence during the rapid climate oscillations of the last deglaciation, T_{dw} and Greenland temperatures have remained well coupled, indicating major changes in deep-water hydrography in association with these millennial events. Similar though less pronounced millennial-scale T_{dw} changes are also exhibited in MD99-2334K during the glaciation in association with the ice-rafting pulses that correspond to Heinrich events 3, 2 and 1 (Figure 5). Thus Heinrich events 3 and 2, and the Younger Dryas each mark the end of a period of relatively warm T_{dw}, and a transition to lower T_{dw} and $\delta^{18}O_{dw}$ conditions. During the period ~17.5–15 cal. ka BP, when increasing ice-rafting in the North Atlantic eventually culminated in Heinrich event 1 [*Elliot et al.*, 1998; *Labeyrie et al.*, 1999], T_{dw} remained relatively warm though unstable, exhibiting a series of intense transient reductions despite a gradual increase from ~17.5 cal. ka BP.

[17] Although there is not a perfect match between Greenland and deep-water temperatures throughout the last ~34 ka (correlation coefficient $R^2 \sim 0.72$), potentially due to the large degree of noise in the T_{dw} record, the apparent correspondence of Greenland stadials with IRD events and decreasing T_{dw} and $\delta^{18}O_{dw}$ in MD99-2334K may reflect a coupling of atmospheric and deep-water temperatures in the North Atlantic via active NADW formation and export. On this conceptual basis, the T_{dw} and Greenland temperature records would share a common component of variability due to variations in NADW formation, and the T_{dw} record from MD99-2334K would represent the changing influence of NADW on local deep-water temperature, though not necessarily the temperature or the flux of NADW alone. This interpretation draws support from a comparison of parallel changes in T_{dw} and $\delta^{18}O_{dw}$ recorded in MD99-2334K, discussed below.

6.3. T_{dw} and $\delta^{18}O_{dw}$: NADW-AABW Mixing

[18] Throughout MD99-2334K, millennial-scale T_{dw} and $\delta^{18}O_{dw}$ changes remain closely coupled, resulting in an alternation between cold, low-$\delta^{18}O_{dw}$ versus warmer, high-$\delta^{18}O_{dw}$ conditions. The covariance of T_{dw} and $\delta^{18}O_{dw}$ in MD99-

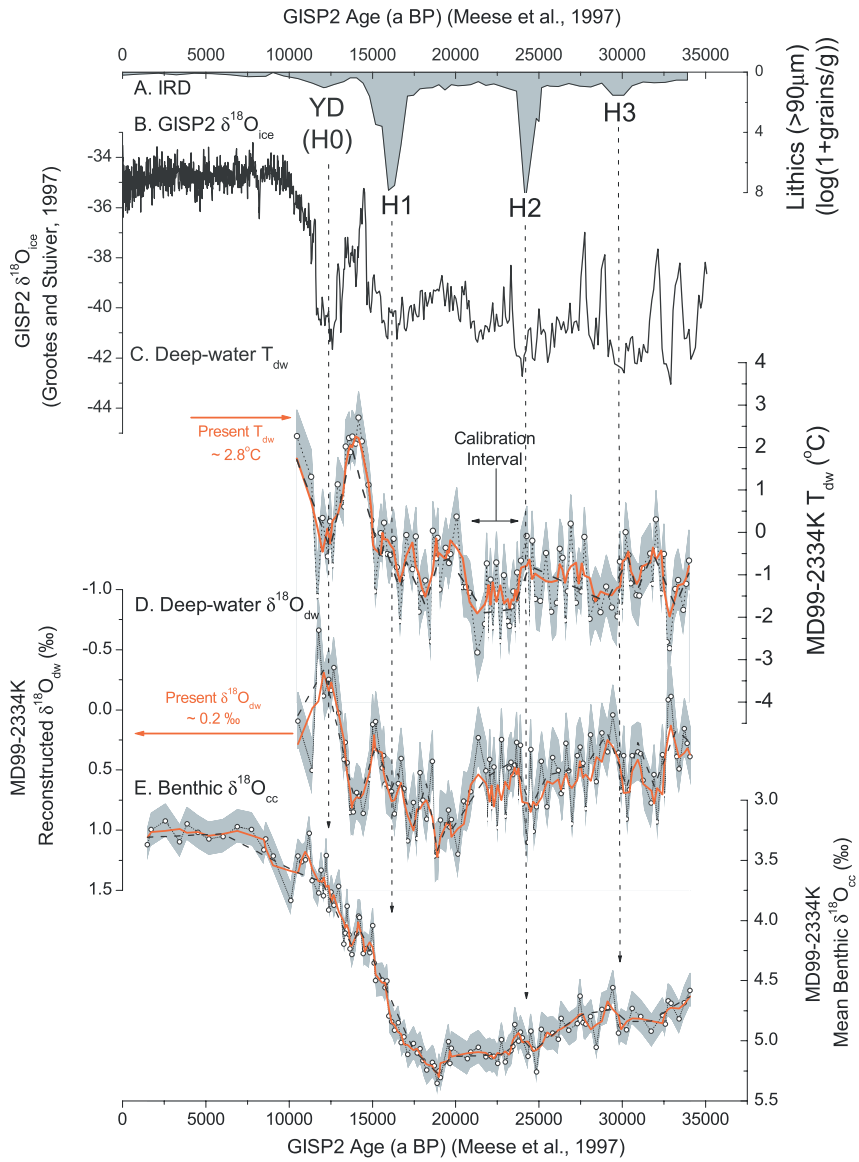

Figure 5. Down-core results from MD99-2334K on the GISP2 age-scale [*Meese et al.*, 1997]. (a) Terrigenous clastic concentration (IRD) >90 μm (on reversed logarithmic scale). (b) GISP2 $\delta^{18}O_{ice}$ [*Grootes and Stuiver*, 1997; *Meese et al.*, 1997]. (c) Deep-water temperature based on Mg/Ca measurements in *G. affinis* (see text for calibration details). (d) Reconstructed deep-water $\delta^{18}O_{dw}$, derived from paired T_{dw} estimates and mean corrected benthic $\delta^{18}O_{cc}$ measurements using the palaeotemperature equation of *O'Neil et al.* [1969] [*O'Neil et al.*, 1969; *Shackleton*, 1974]. (e) Mean corrected benthic $\delta^{18}O_{cc}$ based on measurements in *G. affinis* and *P. wuellerstorfii*, corrected for their respective equilibrium offsets [*Shackleton et al.*, 2000]. In Figures 5c, 5d, and 5e, open circles represent the raw data, and shaded grey areas represent the estimated uncertainty in the records (based on average deviation of adjacent measurements); red lines represent 3-point smoothing; and black dashed lines indicates the statistically significant changes identified in the records (for 90% two-tailed confidence intervals) using t-tests for the difference across 5-point intervals. The inflection points in the black dashed lines thus indicate the timing of significant changes in the records (between inflection points the dashed lines do not represent data values).

2334K is similar to that in the modern deep Atlantic, where T_{dw} and $\delta^{18}O_{dw}$ conditions are determined by the relative proportions of warmer, high-$\delta^{18}O_{dw}$ North Atlantic Deep Water (NADW) versus colder, low-$\delta^{18}O_{dw}$ Antarctic Bottom Water (AABW) [*Levitus*, 1994]. As shown in Figure 6a, the relationship between T_{dw} and $\delta^{18}O_{dw}$ changes recorded in MD99-2334K is consistent with the

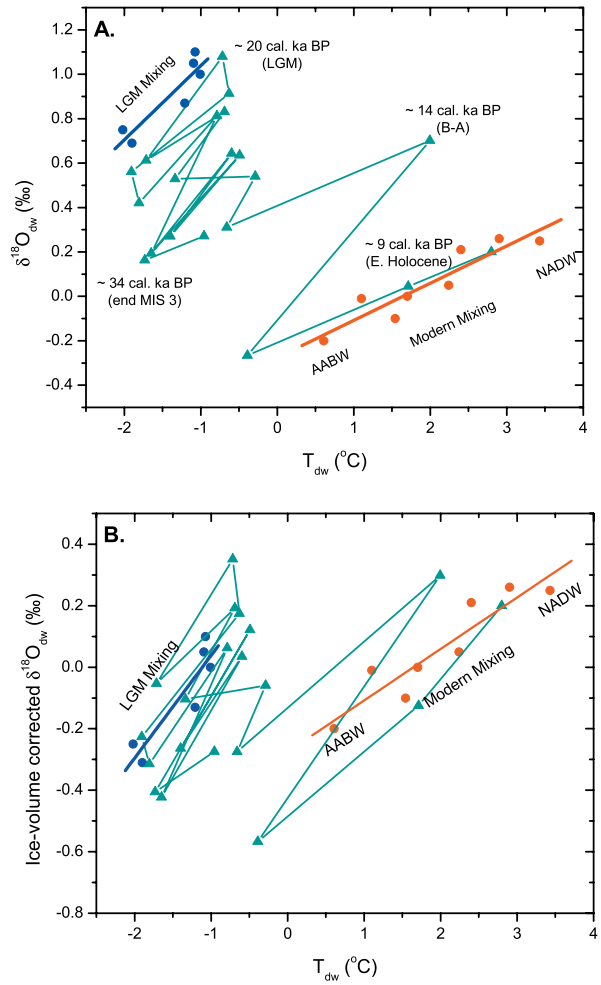

Figure 6. (a) Evolution of T_{dw} and $\delta^{18}O_{dw}$ conditions recorded in MD99-2334K. Solid triangles represent 3-point smoothed data points on either side of 5-point data runs that define significant changes in the data series (see text). The possibility for $\delta^{18}O_{dw}$ changes that are purely the result of noise in the T_{dw} data is thus minimized ($\delta^{18}O_{dw}$ changes of less than ~0.12‰ may be imposed by noise in the smoothed T_{dw} record). Dates indicate approximate timing of the associated T_{dw}-$\delta^{18}O_{dw}$ conditions. Closed circles represent in situ T_{dw} and $\delta^{18}O_{dw}$ values measured in the modern deep Atlantic and inferred for the LGM based on pore water estimates of LGM $\delta^{18}O_{dw}$ and benthic $\delta^{18}O_{cc}$ measurements [*Zahn and Mix*, 1991; *Adkins et al.*, 2002; *Duplessy et al.*, 2002]. Lines fit to these data points represent mixing lines between the northern and southern end-members. (b) As for Figure 6a with $\delta^{18}O_{dw}$ values corrected for the current best estimate of the maximum ice-volume component at millennial timescales, using data compiled by *Lambeck and Chappell* [2001] and reconstructed by *Siddall et al.* [2003], which have been scaled to maximum 1.0‰ glacial – interglacial $\delta^{18}O_{dw}$ change [*Schrag et al.*, 2002].

slope of the present deep Atlantic T-$\delta^{18}O$ mixing line defined by NADW and AABW end-members, and also corresponds closely to the last glacial maximum (LGM) mixing line that may be inferred from combined pore water estimates of LGM $\delta^{18}O_{dw}$ and LGM benthic $\delta^{18}O_{cc}$ measurements from the deep Atlantic, Southern Ocean and Pacific [*Zahn and Mix*, 1991; *Adkins et al.*, 2002; *Duplessy et al.*, 2002]. Hence the millennial T_{dw} and $\delta^{18}O_{dw}$ variations reconstructed in MD99-2334K may be explained by changes in the extent of NADW - AABW mixing.

[19] However, two issues must be addressed in regard to the T_{dw} – $\delta^{18}O_{dw}$ variations illustrated in Figure 6a. Firstly, the positive correlation of T_{dw} and $\delta^{18}O_{dw}$ in both the modern and LGM Atlantic, and in addition the similarity of the deep Atlantic T_{dw} – $\delta^{18}O_{dw}$ slope to the that of the palaeotemperature equation (both close to ~0.2‰ $°C^{-1}$), makes it inherently difficult to test the validity of reconstructed T_{dw} – $\delta^{18}O_{dw}$ relationships. This is because true deep Atlantic T_{dw} – $\delta^{18}O_{dw}$ variations are indistinguishable from the effect of spurious T_{dw} estimates that have been "imposed" on an invariant $\delta^{18}O_{cc}$ record. Thus uncertainties in the Mg/Ca-temperature calibration, both due to scatter in the calibration data and due to uncertainty in the assumptions regarding the range of glacial - interglacial temperature changes (i.e., changing from near freezing to modern) will tend to enhance any real covariance between past T_{dw} and $\delta^{18}O_{dw}$ that might be reconstructed. In Figure 6a, the estimated uncertainties in the temperature calibration and Mg/Ca record may enhance apparent (smoothed) $\delta^{18}O_{dw}$ changes by as much as ~0.09‰, potentially accounting for ~30% (though critically not 100%) of the most statistically significant $\delta^{18}O_{dw}$ variations (see Figure 5). The positive correlation of T_{dw} estimates with the "forced noise" they may incur in $\delta^{18}O_{dw}$ reconstructions, paralleling the positive correlation of *real* T_{dw} and $\delta^{18}O_{dw}$ conditions in the deep Atlantic, represents an inherent difficulty that underlines the importance of obtaining additional constraints from "palaeo-tracer" proxies, such as carbon or neodymium isotopes [*Rutberg et al.*,

2000], without which changes in the sourcing of deep-water cannot be unequivocally resolved.

[20] The second major uncertainty inherent in the T_{dw} – $\delta^{18}O_{dw}$ variations illustrated in Figure 6a is the contribution of millennial sea level fluctuations to $\delta^{18}O_{dw}$ excursions. Although the glacial – interglacial ice-volume component amounts to a ~1.0 ± 0.1‰ change in $\delta^{18}O_{dw}$ [*Labeyrie et al.*, 1987; *Adkins et al.*, 2002], the contribution of millennial glacioeustatic variations remains poorly constrained. Thus changes in glacioeustacy and deep-water hydrography have both been invoked as valid explanations for millennial benthic $\delta^{18}O_{cc}$ variations identified in the geological record [*Rassmussen et al.*, 1996; *Vidal et al.*, 1997; *Lund and Mix*, 1998; *Vidal et al.*, 1998; *Shackleton et al.*, 2000]. Current estimates of sea level change during the last glaciation, based on coral terrace facies [*Chappell*, 2002] and salinity variations in the Red Sea [*Siddall et al.*, 2003], suggest that a significant portion of millennial variations recorded in the Northeast Atlantic benthic $\delta^{18}O_{cc}$ record [*Shackleton et al.*, 2000] may be attributable to rapid changes in ice-volume during Marine Isotope Stage (MIS) 3. However if correct, these same sea level estimates also require an additional component of variability in the Northeast Atlantic benthic $\delta^{18}O_{cc}$ record that must be attributed to local changes in deep-water hydrography, though which occurred in concert with sea level fluctuations [*Chappell*, 2002; *Siddall et al.*, 2003].

[21] Hence a maximum estimate of the glacioeustatic component of the $\delta^{18}O_{dw}$ record from MD99-2334K may be provided by pooled data from *Lambeck and Chappell* [2001] (on an independent calendar time-scale) and from *Siddall et al.* [2003] (placed on a calendar time-scale that maximizes the contribution of reconstructed ice-volume fluctuations to the deep Northeast Atlantic benthic $\delta^{18}O_{cc}$ record). The resulting sea level record may be scaled to a net glacioeustatic $\delta^{18}O_{dw}$ change of 1.0‰ for minimum glacial sea level [*Schrag et al.*, 2002], and thus removed from marine $\delta^{18}O$ measurements. This is illustrated in Figure 6b for the $\delta^{18}O_{dw}$ record from MD99-2334K, where after accounting for the maximum current estimates of changing ice-volume, the reconstructed T_{dw} and $\delta^{18}O_{dw}$ variations remain indicative of the repeated alternation between two relatively invariant deep-water end-members that are analogous to, though much colder than, the modern NADW and AABW end-members.

[22] In Figure 7, the same approach is extended to a comparison of the $\delta^{18}O_{dw}$ record from MD99-2334K with the inferred non-glacioeustatic component of the benthic $\delta^{18}O_{cc}$ record from the neighboring core MD95-2042 [*Shackleton et al.*, 2000]. Thus millennial variations in benthic $\delta^{18}O_{cc}$ that are well resolved in core MD95-2042 cannot be completely accounted for by current estimates of global ice-volume fluctuations, and must therefore correspond to local hydrographic change. The $\delta^{18}O_{dw}$ record from MD99-2334K suggests that these changes are dominated by coupled and positively correlated T_{dw} and $\delta^{18}O_{dw}$ changes, suggested in Figure 6 to represent the changing dominance of different deep-water sources.

6.4. A Bi-Polar "See-Saw"?

[23] If the millennial T_{dw} and $\delta^{18}O_{dw}$ excursions recorded in MD99-2334K are taken to represent at least in part the effect of changes in the extent of NADW-AABW mixing, then the negative excursions in $\delta^{18}O_{dw}$ record, which are also apparent in the benthic $\delta^{18}O_{cc}$ record (Figures 5 and 7) and which coincide with Greenland stadial events and local ice-rafting pulses (in particular the Younger Dryas, or H0), would in part represent the increased influence of AABW (with respect to NADW) in the deep Northeast Atlantic. These incursions of AABW appear to have resulted generally, though not exclusively, from fresh-water forced NADW collapse, and may have involved a concomitant increase in the export of AABW [*Broecker*, 1998; *Seidov and Maslin*, 2001; *Weaver et al.*, 2003]. These interpretations lend support to oscillatory thermohaline circulation models that generate asynchronous inter-hemispheric climate variability as a result of the changing relative stability of northern- and southern sourced deep-waters [*Broecker*,

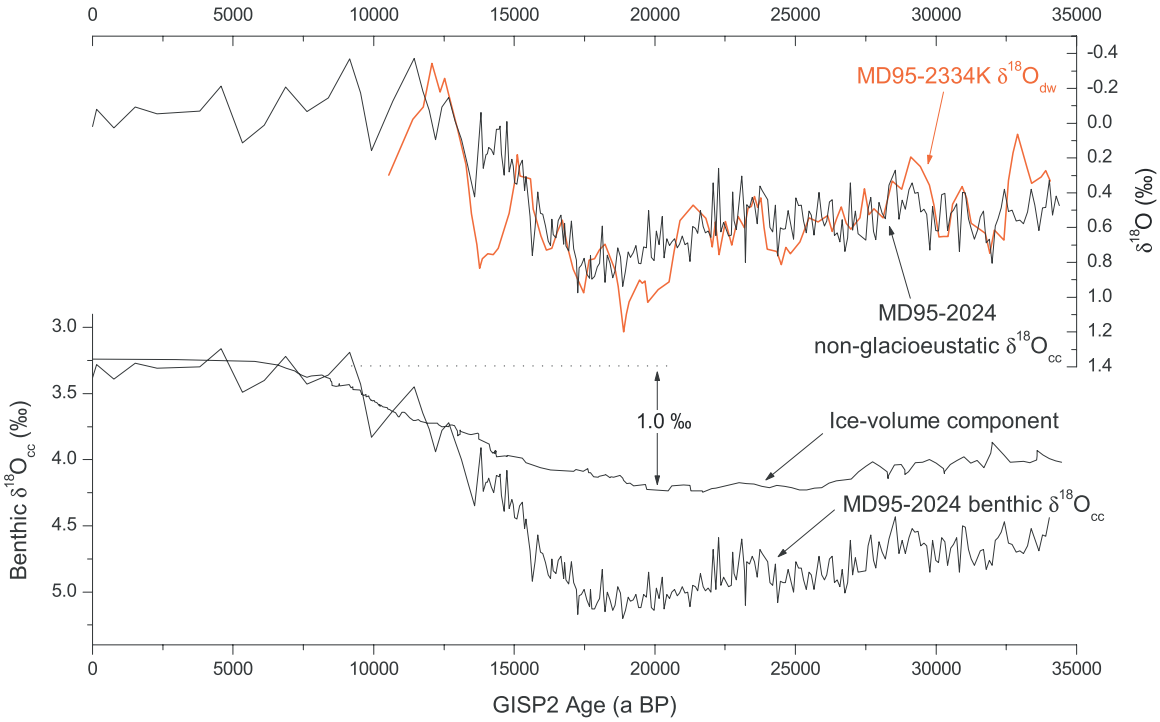

Figure 7. Comparison of the non-glacioeustatic component of the benthic $\delta^{18}O_{cc}$ record from core MD95-2042 [*Shackleton et al.*, 2000], with the $\delta^{18}O_{dw}$ record from MD99-2334K (this study). Both cores are from the same location on the Iberian Margin. In the lower plot, the ice volume component is derived as in Figure 6b (see text). In the upper plot, the nonglacioeustatic component of the MD95-2042 $\delta^{18}O_{cc}$ record (black line) represents the difference between the two curves illustrated in the lower plot, and closely resembles the $\delta^{18}O_{dw}$ record from MD99-2334K (red line), indicating a common component due to local deep-water change.

1998; *Seidov and Maslin*, 2001; *Weaver et al.*, 2003].

[24] One interesting feature of the T_{dw} record from MD99-2334K is the apparent warming of deep-waters from ~22 cal. ka BP. This warming is a robust feature of the T_{dw} record (significant for a 99% t-test confidence interval) and occurs in parallel with warming over Greenland (Figure 4), though also during a time of increasing ice-rafting and deteriorating climate in the North Atlantic which eventually culminated in Heinrich event 1 [*Chapman and Shackleton*, 1998; *Elliot et al.*, 1998; *Labeyrie et al.*, 1999]. This implies a degree of de-coupling between NADW stability (linked to Greenland temperatures) and surface water conditions in the North Atlantic, and may indicate an important stabilising mechanism for NADW formation (or at least the deep-Atlantic heat budget) that was insensitive to high northern latitude surface water conditions in the late glacial. The stability of AABW formation, and hence perhaps of the Antarctic ice sheet [*Kanfoush et al.*, 2000; *Clark et al.*, 2002], may have played a role in such a mechanism, as suggested by recent modeling experiments for the Bølling-Allerød warming [*Weaver et al.*, 2003].

[25] These results have a direct bearing on the observed asynchrony between Greenland and Antarctic records of millennial climate change [*Blunier and Brook*, 2001]. Indeed the most pronounced and unambiguous changes in T_{dw} and $\delta^{18}O_{dw}$ reconstructed in MD99-2334K occurred in parallel with the Bølling-Allerød and Younger Dryas events, both of which were accompanied by contrasting climatic counterparts in Antarctica [*Blunier and Brook*, 2001]. Thus Figure 8 illustrates how the asynchrony identified between T_{dw} and $\delta^{18}O_{dw}$ variations in the deep Northeast Atlantic, based on the data from MD99-2334K, runs parallel to the asynchrony of

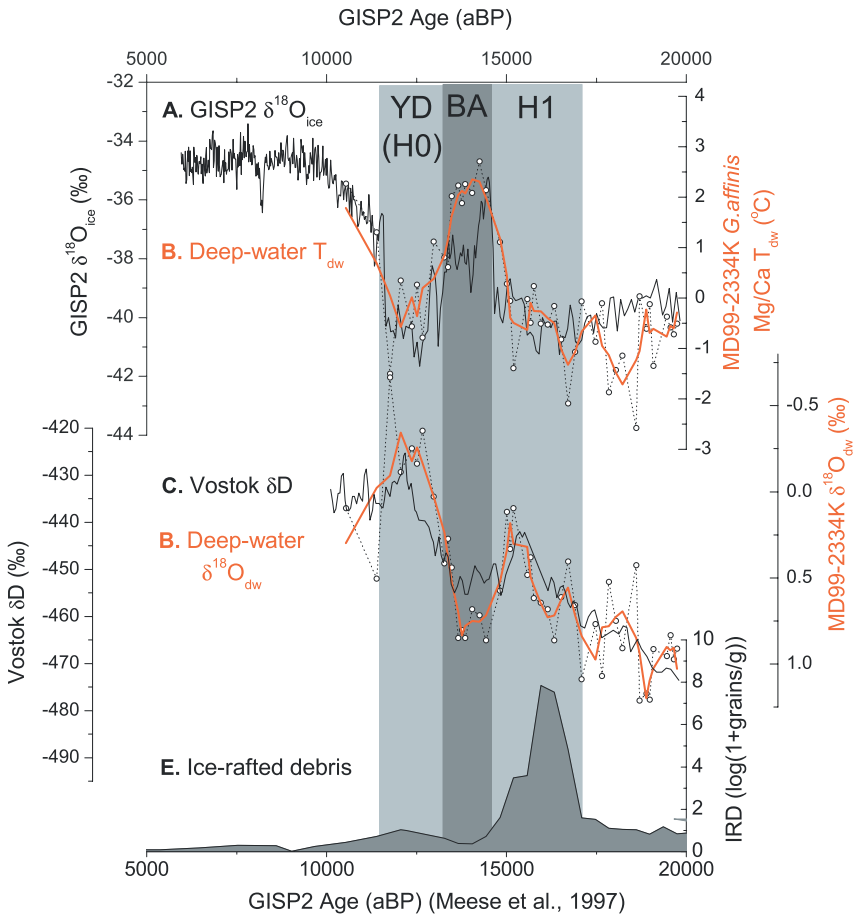

Figure 8. Changes in T_{dw} and $\delta^{18}O_{dw}$ reconstructed in MD99-2334K across the last deglaciation, compared with climate changes recorded in the Greenland and Antarctic ice cores. (a) GISP2 $\delta^{18}O_{ice}$ data from *Grootes and Stuiver* [1997]. (b) T_{dw} data from MD99-2334K, thick red line represents 3-point smoothed version. (c) Vostok δD data from *Johnsen et al.* [1972], synchronized to the GISP2 record via the correlation of the GRIP and GISP2 records and the synchronized GRIP age-scale of *Blunier et al.* [2001]. (e) Ice-rafted debris concentrations in MD99-2334K. All records are thus plotted on the GISP2 age-scale of *Meese et al.* [1997].

Greenland and Antarctic climate change across the last deglaciation, suggesting an important role for the meridional overturning cell in these global climatic events.

7. Conclusions

[26] Paired measurements of Mg/Ca and $\delta^{18}O_{cc}$ in benthic foraminifera from core MD99-2334K indicate a marked reduction of deep-water temperatures in the Northeast Atlantic during the last glaciation and suggest a coupling of T_{dw} with Greenland climate at millennial time-scales, in particular across the Bølling-Allerød and Younger Dryas climate oscillations. Indeed, at millennial time-scales, reconstructed $\delta^{18}O_{dw}$ and T_{dw} variations consistently co-vary throughout the last ~34 cal. ka, suggesting the changing relative influence of warmer, high-$\delta^{18}O_{dw}$ NADW versus colder, low-$\delta^{18}O_{dw}$ AABW. Perturbations to T_{dw} and $\delta^{18}O_{dw}$, and hence the relative mixing of NADW and AABW, appear to be linked to pulses of ice-rafting accompanying Heinrich events 3, 2, 1 and the Younger Dryas, when punctuated changes to colder, low-$\delta^{18}O_{dw}$ conditions were incurred. Hence the observed similarity of T_{dw} and Greenland temperature variations may reflect a common component of variability resulting from changes in the export of NADW to the deep Northeast Atlantic. Because T_{dw} and $\delta^{18}O_{dw}$ in MD99-2334K

are linked via the exchange of NADW and AABW dominance in the Northeast Atlantic, the $\delta^{18}O_{dw}$ and benthic $\delta^{18}O_{cc}$ records bear a millennial AABW signal whose relation to Greenland climate is determined by the link between Greenland climate and thermohaline stability, which may not only be sensitive to freshwater forcing in the high northern latitudes.

Acknowledgments

[27] We record out thanks for the expert assistance of Mike Hall, James Rolfe and Mervyn Greaves, and the helpful advice of Isabel Cacho. We are also very grateful to Laurent Labeyrie and Eelco Rohling, whose comments greatly improved this manuscript. This work has been undertaken in association with the ''POP Project'', EC Grant EVK2-2000-00089, NERC grant GR3/12889, and an award from the Comer Foundation.

References

Adkins, J. F., K. McIntyre, and D. P. Schrag, The salinity, temperature and $\delta^{18}O$ of the glacial deep ocean, *Science*, *298*, 1769–1773, 2002.

Anand, P., H. Elderfield, and M. H. Conte, Calibration of Mg/Ca thermometry in planktonic foraminifera from a sediment trap time series, *Paleoceanography*, *18*(2), 1050, doi:10.1029/2003PA000846, 2003.

Bard, E., M. Arnold, J. Duprat, J. Moyes, and J.-C. Duplessy, Reconstruction of the last deglaciation: Deconvolved records of $\delta^{18}O$ profiles, micropalaeontological variations and accelerator mass spectrometric ^{14}C dating, *Clim. Dyn.*, *1*, 101–112, 1987.

Bard, E., B. Hamelin, R. G. Fairbanks, and A. Zindler, Calibration of the ^{14}C timescale over the past 30,000 years using mass spectrometric U-Th ages from Barbados corals, *Nature*, *345*, 405–409, 1990.

Barker, S., M. Greaves, and H. Elderfield, A study of cleaning procedures used for foraminiferal Mg/Ca paleothermometry, *Geochem. Geophys. Geosyst.*, *4*(9), 8407, doi:10.1029/2003GC000559, 2003.

Blunier, T., and E. J. Brook, Timing of millennial-scale climate change in Antarctica and Greenland during the last glacial period, *Science*, *291*, 109–112, 2001.

Blunier, T., et al., Asynchrony of Antarctic and Greenland climate change during the last glacial period, *Nature*, *394*, 739–743, 1998.

Boyle, E. A., Manganese carbonate overgrowths on foraminifera tests, *Geochim. Cosmochim. Acta*, *47*, 1815–1819, 1983.

Boyle, E. A., Is ocean circulation linked to abrupt stadial/interstadial transitions?, *Quat. Sci. Rev.*, *19*, 255–272, 2000.

Broecker, W. S., Massive iceberg discharges as triggers for global climate change, *Nature*, *372*, 421–424, 1994.

Broecker, W. S., Palaeocean circulation during the last deglaciation: A bipolar seesaw?, *Paleoceanography*, *13*, 119–121, 1998.

Brown, S. J., and H. Elderfield, Variations in Mg/Ca and Sr/Ca ratios in planktonic foraminifera caused by postdepositional dissolution: Evidence of shallow Mg-dependent dissolution, *Paleoceanography*, *11*, 543–551, 1996.

Chapman, M. R., and N. J. Shackleton, Millennial-scale fluctuations in North Atlantic heat flux during the last 150,000 years, *Earth Planet. Sci. Lett.*, *159*, 57–70, 1998.

Chappell, J., Sea level changes forced ice breakouts in the Last Glacial cycle: New results form coral terraces, *Quat. Sci. Rev.*, *21*, 1229–1240, 2002.

Charles, C. D., J. Lynch-Stieglitz, U. S. Ninneman, and R. G. Fairbanks, Climate connections between the hemispheres revealed by deep sea sediment core/ice core correlations, *Earth Planet. Sci. Lett.*, *142*, 19–42, 1996.

Clark, P. U., J. X. Mitrovica, G. A. Milne, and M. E. Tamisea, Sea-level fingerprinting as a direct test for the source of global meltwater pulse IA, *Science*, *295*, 2438–2441, 2002.

de Lange, G. J., B. van Os, and R. Poorter, Geochemical composition and inferred accretion rates of sediments and manganese nodules from a submarine hill in the Madeira Abyssal Plain, eastern North Atlantic, *Mar. Geol.*, *109*, 171–194, 1992.

de Villiers, S., M. Greaves, and H. Elderfield, An intensity ratio calibration method for the accurate determination of Mg/Ca and Sr/Ca of marine carbonates by ICP-AES, *Geochem. Geophys. Geosyst.*, *3*, 1001, doi:10.1029/2001GC000169, 2002.

Duplessy, J.-C., et al., Deep water source variations during the last climatic cycle and their impact on global deep water circulation, *Paleoceanography*, *3*, 343–360, 1988.

Duplessy, J.-C., L. Labeyrie, and C. Waelbroeck, Constraints on the ocean oxygen isotopic enrichment between the Last Glacial Maximum and the Holocene: Palaeoceanographic implications, *Quat. Sci. Rev.*, *21*, 315–350, 2002.

Dwyer, G. S., T. M. Cronin, P. A. Baker, and J. Rodriguez-Lazaro, Changes in North Atlantic deep-sea temperature during climatic fluctuations of the last 25,000 years based on ostracode Mg/Ca ratios, *Geochem. Geophys. Geosyst.*, *2*, Paper number 2000GC000046, 2000.

Edwards, R. L., H. Cheng, M. T. Murrell, and S. J. Goldstein, Protactinium-231 dating of carbonates by thermal ionization mass spectromotry: Implications for Quaternary climate change, *Science*, *276*, 782–786, 1997.

Elderfield, H., and G. Ganssen, Past Temperature and $\delta^{18}O$ of surface ocean waters inferred from foraminiferal Mg/Ca ratios, *Nature*, *405*, 442–445, 2000.

Elliot, M., et al., Millennial-scale iceberg discharges in the Irminger Basin during the last glacial period: Relationship with Heinrich events and environmental settings, *Paleoceanography*, *13*, 433–446, 1998.

Gallup, C., H. Cheng, F. W. Taylor, and R. L. Edwards, Direct determination of the timing of sea level change during Termination II, *Science*, *295*, 310–313, 2002.

Grootes, P. M., and M. Stuiver, Oxygen 18/16 variability in Greenland snow and ice with 10^3 to 10^5-year time resolution, *J. Geophys. Res.*, *102*, 26,455–26,470, 1997.

Johnsen, S. J., D. Dansgaard, H. B. Clausen, and C. C. Langway Jr., Oxygen isotope profiles through the Antarctic and Greenland ice sheets, *Nature*, *235*, 429–434, 1972.

Kanfoush, S. L., et al., Millennial-scale instability of the Antarctic ice sheet during the last glaciation, *Science*, *288*, 1815–1818, 2000.

Labeyrie, L., J. C. Duplessy, and P. L. Blanc, Variations in mode of formation and temperature of oceanic deep waters over the past 125,000 years, *Nature*, *327*, 477–482, 1987.

Labeyrie, L., H. Leclaire, C. Waelbroeck, E. Cortijo, J. C. Duplessy, L. Vidal, M. Elliot, B. Lecoat, and G. Aufret, Temporal variability of the Surface and Deep Waters of the northwest Atlantic Ocean at Orbital and Millennial Scales, in *Mechanisms of Millennial-Scale Climate Change*, *Geophys. Monogr. Ser.*, vol. 112, edited by P. U. Clark, R. S. Webb, and L. D. Keigwin, pp. 77–98, AGU, Washington, D.C., 1999.

Lambeck, K., and J. Chappell, Sea level change through the last glacial cycle, *Science*, *292*, 679–686, 2001.

Lea, D. W., T. A. Mashiotta, and H. J. Spero, Controls on magnesium and strontium uptake in planktic foraminifera determined by live culturing, *Geochim. Cosmochim. Acta*, *63*, 2369–2379, 1999.

Lea, D. W., D. K. Pak, and H. J. Spero, Climate impact of late Quaternary equatorial Pacific Sea surface temperature variations, *Science*, *289*, 1719–1724, 2000.

Lear, C. H., H. Elderfield, and P. A. Wilson, Cenozoic deep-sea temperatures and global ice volumes from Mg/a in benthic foraminiferal calcite, *Science*, *287*, 269–272, 2000.

Lear, C. H., Y. Rosenthal, and N. Slowey, Benthic foraminiferal Mg/Ca-paleothermometry: A revised core-top calibration, *Geochim. Cosmochim. Acta*, *66*, 3375–3387, 2002.

Levitus, S., *World Ocean Atlas*, Natl. Oceanic and Atmos. Admin., Washington, D. C., 1994.

Lund, D. C., and A. C. Mix, Millennial-scale deep water oscillations: Reflections of the North Atlantic in the deep Pacific from 10 to 60 ka, *Paleoceanography*, *13*, 10–19, 1998.

Martin, P. A., et al., Quaternary deep sea temperature histories derived from benthic foraminiferal Mg/Ca, *Earth Planet. Sci. Lett.*, *198*, 193–209, 2002.

Mashiotta, T. A., D. W. Lea, and H. J. Spero, Glacial-interglacial changes in Subantarctic sea surface temperature and d18O-water using foraminiferal Mg, *Earth Planet. Sci. Lett.*, *170*, 417–432, 1999.

Meese, D. A., et al., The Greenland Ice Sheet Project 2 depth-age scale: Methods and results, *J. Geophys. Res.*, *102*, 26,411–26,423, 1997.

Nürnberg, D., Magnesium in tests of *Neogloboquadrina pachyderma* sinistral from high northern and southern latitudes, *J. Foraminiferal Res.*, *25*, 350–368, 1995.

Nürnberg, D., J. Bijma, and C. Hemleben, Assessing the reliability of magnesium in foraminiferal calcite as a proxy for water mass temperatures, *Geochim. Cosmochim. Acta*, *60*, 803–814, 1996a.

Nürnberg, D., J. Bijma, and J. Hemleben, Assessing the reliability of magnesium inforaminiferal calcite as a proxy for water mass temperatures, *Geochim. Cosmochim. Acta*, *60*, 803–814, 1996b.

O'Neil, J. R., R. N. Clayton, and T. K. Mayeda, Oxygen isotope fractionation in divalent metal carbonates, *J. Chem. Phys.*, *51*, 5547–5558, 1969.

Rassmussen, T. L., E. Thomsen, T. C. E. van Weering, and L. Labeyrie, Rapid changes in surface and deep-water conditions at the Faroe Margin during the last 85,000 years, *Paleoceanography*, *11*, 71–757, 1996.

Rosenthal, Y., E. Boyle, and N. Slowey, Temperature control on the incorporation of magnesium, strontium, fluorine, and cadmium into benthic foraminiferal shells from Little Bahama Bank: Prospects for thermocline palaeoceanography, *Geochim. Cosmochim. Acta*, *61*, 3633–3643, 1997.

Rosenthal, Y., G. P. Lohmann, K. C. Lohmann, and R. M. Sherrell, Incorporation and preservation of Mg in *Globigerinoides succulifer*: Implications for reconstructing the temperature and 18O/16O of seawater, *Paleoceanography*, *15*, 135–145, 2000.

Rutberg, R. L., S. R. Heming, and S. L. Goldstein, Reduced North Atlantic Deep Water flux to the glacial Southern Ocean inferred from neodymium isotope ratios, *Nature*, *405*, 935–938, 2000.

Schrag, D. P., et al., The oxygen isotopic composition of seawater during the Last Glacial Maximum, *Quat. Sci. Rev.*, *21*, 331–342, 2002.

Seidov, D., and M. Maslin, Atlantic Ocean heat piracy and the bipolar climate see-saw during Heinrich and Dansgaard-Oeschger events, *J. Quat. Sci.*, *16*, 321–328, 2001.

Shackleton, N. J., Attainment of isotopic equilibrium ocean water and the benthonic foraminifera genus *Uvigerina*: Isotopic changes in the ocean during the last glacial, *Cent. Natl. Rech. Sci. Colloq. Int.*, *219*, 203–209, 1974.

Shackleton, N. J., M. A. Hall, and E. Vincent, Phase relationships between millennial-scale events 64,000–24,000 years ago, *Paleoceanography*, *15*, 565–569, 2000.

Shackleton, N. J., M. F. Sanchez-Goni, D. Pailler, and Y. Lancelot, Marine isotope substage 5e and the Eemian interglacial, *Global Planet. Change*, *757*, 1–5, 2003.

Siddall, M., E. Rohling, A. Almogi-Labin, C. Hemleben, D. Meischner, I. Schmelzer, and D. A. Smeed, Sea-level fluctuations during the last glacial cycle, *Nature*, *423*, 853–858, 2003.

Stirling, C. H., T. M. Esat, K. Lambeck, and M. T. McCulloch, Timing and duration of the Last Interglacial: Evidence for a restricted interval of widespread coral reef growth, *Earth Planet. Sci. Lett.*, *160*, 745–762, 1998.

Stocker, T. F., D. G. Wright, and W. S. Broecker, The influence of high latitude surface forcing on the global thermohaline circulation, *Paleoceanography*, *7*, 529–542, 1992.

Tachikawa, K., C. Fontanier, F. Jorissen, and E. Bard, *Mg/Ca and Sr/Ca in living benthic foraminiferal tests from the Northeastern Atlantic*, paper presented at the EGS-AGU-

EUG Joint Assembly, Eur. Geophys. Soc., Nice, France, 2003.

Toyofuku, T., H. Kitazato, H. Kawahata, M. Tsuchiya, and M. Nohara, Evaluation of Mg/Ca thermometry in foraminifera: Comparison of experimental results and measurements in nature, *Paleoceanography*, *15*, 456–464, 2000.

van Aken, H., The hydrography of the mid-latitude northeast Atlantic Ocean I: The deep water masses, *Deep Sea Res. I*, *47*, 757–787, 2000.

Vidal, L., et al., Evidence for changes in the North Atlantic Deep Water linked to meltwater surges during Heinrich events, *Earth Planet. Sci. Lett.*, *146*, 13–27, 1997.

Vidal, L., L. Labeyrie, and T. C. E. van Weering, Benthic $\delta^{18}O$ records in the North Atlantic over the last glacial period (60–10 kyr): Evidence for brine formation, *Paleoceanography*, *13*, 245–251, 1998.

Voelker, A. H. L., P. M. Grootes, M.-J. Nadeau, and M. Sarnthein, Radiocarbon levels in the Iceland Sea from 25–53 kyr and their links to the earth's magnetic field intensity, *Radiocarbon*, *42*, 437–452, 2000.

Weaver, A. J., O. A. Saenko, P. U. Clark, and J. X. Mitrovica, Meltwater pulse 1A from Antarctica as a trigger for the Bolling-Allerod warm interval, *Science*, *299*, 1709–1713, 2003.

Zahn, R., and A. C. Mix, Benthic foraminiferal d18O in the ocean's temperature-salinity-density field: Constraints on ice age thermohaline circulation, *Paleoceanography*, *6*, 1–20, 1991.